

熔化极气体保护焊的直接自适应控制

张 涛, 桂卫华, 王随平

(中南大学 信息科学与工程学院, 湖南 长沙 410083)

摘 要: 焊接电流和电弧长度是熔化极气体保护焊 (GMAW) 焊接过程的主要状态变量, 决定了熔滴的过渡过程、热量输入和焊缝成形. 文中在分析 GMAW 焊接工艺过程的基础上, 建立了焊接电流和电弧长度的数学模型, 采用基于二次型性能指标的直接自适应控制算法, 通过调节焊接电源输出电压和送丝速度的大小, 使焊接电流和电弧长度能跟踪参考模型的输出. 同时, 针对实际应用中难以检测的电弧长度, 建立了电弧长度估计模型, 实现了对电弧长度的软测量. 结果表明, 该算法可以实现弧长和电流的精确控制.

关键词: 熔化极气体保护焊; 直接自适应控制; 弧长估计

中图分类号: TG431.5 文献标识码: A 文章编号: 0253-360X(2010)04-0025-03



张 涛

0 序 言

熔化极气体保护焊 (GMAW) 是一种目前广泛应用的焊接工艺. 在 GMAW 焊接过程中, 焊接电流和感应磁场相互作用, 在熔滴上产生径向的收缩力, 促使熔滴从焊丝上脱落, 熔滴临界尺寸与电流的平方有关, 同时焊接电流也是决定输入热量和焊接质量的最关键的参数^[1]; 因此, 在焊接过程中保证焊接电流的稳定就能保证熔滴过渡的尺寸和均匀性. 另一方面, 在 GMAW 焊接过程中, 维持电弧的稳定燃烧是保证焊接质量的基本条件, 控制器必须在电弧受到波动时, 具有使其回到稳定工作点的能力^[2].

文中采用直接自适应控制算法, 通过调节焊接电源输出电压和送丝速度的大小, 实现 GMAW 过程中焊接电流和电弧长度的控制, 可以根据系统性能选定参考模型, 控制器的设计几乎与被控对象无关.

1 GMAW 焊接过程的模型

GMAW 焊接过程的等效电路如图 1 所示, 由图可得

$$I = \frac{U - [R_s + R_w + \rho(l - l_{rc})] I - U_0 - E_a l_{rc}}{L_s} \quad (1)$$

式中: R_s 为焊接回路输出电阻; R_w 为电弧等效电

阻; ρ 为焊丝电阻率; l 为导电嘴到工件的距离; l_{rc} 为电弧长度; U_0 为弧压常数; E_a 为弧长因子; L_s 为焊接电源输出电感; U 为焊接电源输出电压; I 为焊接电流.

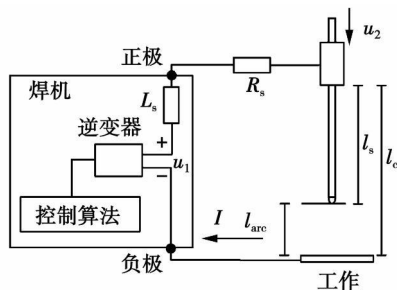


图 1 GMAW 焊接过程的等效电路

Fig. 1 Equivalent circuit of GMAW process

在 GMAW 焊接过程中, 电弧长度的变化与送丝速度 v_f 和焊丝熔化速度 v_m 有关, 焊丝熔化速度 v_m 的模型为^[3]

$$v_m = k_1 I + k_2 \dot{l} (l - l_{rc}) \quad (2)$$

式中: k_1 , k_2 为熔化速度常数. 电弧长度变化模型可表示为

$$\dot{l} = v_f - v_m = v_f - [k_1 I + k_2 \dot{l} (l - l_{rc})] \quad (3)$$

式 (1) 和式 (3) 即为 GMAW 焊接过程电流和电弧长度的动态模型, 可以看出该模型为非线性的, 因此很难应用现代控制理论. 文中将上述微分方程在工作点附近线性化, 并写成状态空间方程的标准形式为

$$\left. \begin{aligned} \begin{bmatrix} \dot{x}_1 \\ \dot{x}_2 \end{bmatrix} &= \begin{bmatrix} \frac{(R_s + R_w + \rho l)}{L_s} & -E_a - \rho \dot{x}_2 \\ k_1 - k_2 \dot{x}_1 l & k_2 \dot{x}_1 \end{bmatrix} \begin{bmatrix} x_1 \\ x_2 \end{bmatrix} + \begin{bmatrix} \frac{1}{L_s} & 0 \\ 0 & 1 \end{bmatrix} \begin{bmatrix} u_1 \\ u_2 \end{bmatrix} \\ \begin{bmatrix} y_1 \\ y_2 \end{bmatrix} &= \begin{bmatrix} 1 & 0 \\ 0 & 1 \end{bmatrix} \begin{bmatrix} x_1 \\ x_2 \end{bmatrix} \end{aligned} \right\} \quad (4)$$

式中： \bar{x}_1 、 \bar{x}_2 分别是状态变量电流和弧长的工作稳态值；系统的输出量 y_1 和 y_2 分别为焊接电流和电弧长度；控制输入量 u_1 和 u_2 分别为焊接电源输出电压和送丝速度。

2 直接参考模型自适应控制算法

被控对象由下述方程描述：

$$\left. \begin{aligned} x_p(k+1) &= A_p x_p(k) + B_p u_p(k) \\ y_p(k) &= C_p x_p(k) \end{aligned} \right\} \quad (5)$$

式中： $y_p(k)$ 为 $(m \times 1)$ 输出矢量； $u_p(k)$ 为 $(m \times 1)$ 控制矢量； $x_p(k)$ 为 $(n_p \times 1)$ 维被控对象状态矢量。 A_p 、 B_p 、 C_p 为具有相应维数的定常矩阵。

参考模型的选择是对系统达到的动态和静态性能的期望，使被控对象跟踪其输出。参考模型可描述为

$$\left. \begin{aligned} x_m(k+1) &= A_m x_m(k) + B_m u_m(k) \\ y_m(k) &= C_m x_m(k) \end{aligned} \right\} \quad (6)$$

式中： $y_m(k)$ 为 $(m \times 1)$ 输出矢量； $u_m(k)$ 为 $(m \times 1)$ 控制矢量； $x_m(k)$ 为 $(n_m \times 1)$ 被控对象状态矢量； A_m 、 B_m 、 C_m 为具有相应维数的定常矩阵。

控制的目的是使被控对象输出渐进跟踪参考模型输出，即

$$\lim_{k \rightarrow \infty} e_y(k) = y_m(k) - y_p(k) = 0 \quad (7)$$

输出跟踪误差为零。

控制律的计算式为^[4]

$$\begin{aligned} u_p(k) &= K_e(k) e_y(k) + K_x(k) x_m(k) + \\ &K_u(k) u_m(k) = K(k) r(k) \end{aligned} \quad (8)$$

式中： K_e 、 K_x 、 K_u 分别为误差变量、状态变量和控制变量的控制算法增益矩阵。当被控对象参数未知时，为了进行自适应控制，控制算法增益矩阵是由自适应律来调节的，采用基于二次型性能指标为最小来确定 $K(k)$ 的自适应调节律，设二次型性能指标为

$$J = \frac{1}{2} [e_y^T(k) P e_y(k) + \Delta u_p^T(k) N \Delta u_p(k)] \quad (9)$$

式中： $P = P^T > 0$ 、 $N = N^T \geq 0$ 分别为跟踪误差和控制增量加权矩阵，使式(9)的性能指标取最小来确定控制参数自适应律，可以在实现对参考模型跟踪的同时又不使控制增量过大。

控制算法增益矩阵 $K(k)$ 的自适应律为

$$K(k+1) = K(k) - \eta \frac{\partial J}{\partial K(k)} = K(k) - \eta [N \Delta u_p(k) r^T(k) r^T(k) - M e_y(k) r^T(k)] \quad (10)$$

式中： η 为适应系数； N 为控制增量加权矩阵； M 为被控对象静态增益矩阵和跟踪误差加权矩阵的乘积，其中参数 N 、 M 和 η 需事先选定。

3 GMAW焊接过程自适应控制器的设计

3.1 系统结构

GMAW焊接过程直接自适应控制系统结构如图2所示，控制律采用基于二次型性能指标计算。 I_d 和 I_{rc} 分别是焊接电流和电弧长度的给定值， I 和 I_{rc} 分别是实际测量值， I_m 和 I_{rcm} 分别是参考模型的焊接电流和电弧长度输出值， e_{y1} 和 e_{y2} 分别是焊接电流和电弧电压的跟踪误差， Z^{-1} 为单位延迟算子，自适应控制器输出矢量 u_p 为电源输出电压和送丝速度，由自适应控制律按照式(8)在线计算调节。

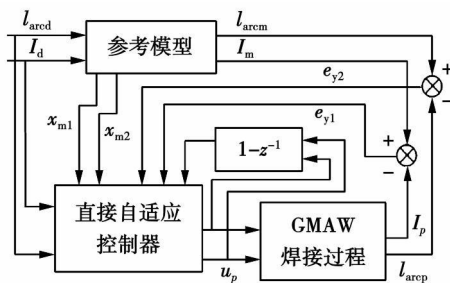


图 2 GMAW直接自适应控制系统结构

Fig 2 Direct model adaptive control structure of GMAW process

3.2 弧长估计模型

控制对象为焊接电流和电弧长度，电流可以通过霍尔电流传感器直接进行检测，但是电弧长度无法直接测量，为此需建立电弧长度估计模型。

在实际焊接系统中，只能检测到焊接电流和焊接电源输出端电压，端电压包括导线压降、焊丝干伸长压降和电弧电压，考虑动态过程的快速性，忽略回路中电感，仅考虑回路电阻，于是焊机输出端电压 u 可以表示为

$$u = (R_w + \rho l_b) I + U_a \quad (11)$$

式中: R_w 是焊接电缆电阻; ρ 是焊丝电阻率; l_b 是焊丝干伸长的预期或平均长度; U_a 为电弧电压。

根据电弧电压与弧长的模型,可以得到弧长估计模型为

$$l_a = \frac{u - (R_w + \rho l_b - R_a) I - U_0}{E_a} \quad (12)$$

3.3 直接自适应控制的设计

在直接自适应控制算法中,参考模型的选取代表对系统性能指标的期望,设计超调量为 10%,峰值时间是 0.05 s;根据这两个期望参数,可求得系统的自然频率和阻尼比,由此将参考模型选为

$$G_m(s) = \frac{Y_m(s)}{U_m(s)} = \frac{6.049}{s^2 + 91.78s + 6.049} \begin{bmatrix} 1 & 0 \\ 0 & 1 \end{bmatrix}$$

自适应算法的参数为

$$\eta = 0.25$$

$$M = \begin{bmatrix} 0.4 & 0.02 \\ 0.03 & 0.5 \end{bmatrix}$$

$$N = \begin{bmatrix} 0.25 & 0 \\ 0 & 0.2 \end{bmatrix}$$

控制增益初值为

$$K(0) = \begin{bmatrix} 0.2 & 0 & 0.1 & 0 & 0.4 & 0 \\ 0 & 0.2 & 0 & 0.1 & 0 & 0.4 \end{bmatrix}$$

3.4 仿真研究

按上面的系统结构,以 GMAW 焊接过程为对象进行仿真研究。仿真中设定弧长的给定值为 7.1 mm,焊接电流给定值为 210 A。仿真结果如图 3 和图 4 所示,可以看出,直接自适应控制的控制输出 $Y_b(k)$ 能很好地跟随参考模型的输出 $Y_m(k)$ 。

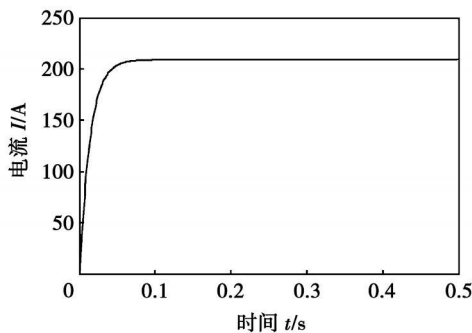


图 3 焊接电流仿真波形

Fig 3 Simulation of welding current

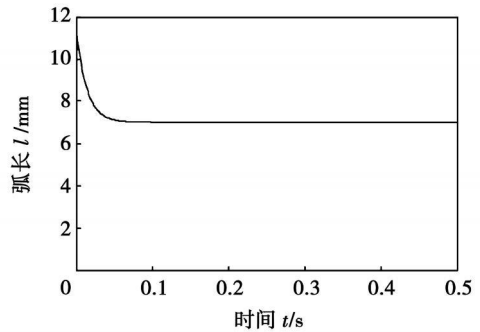


图 4 电弧长度仿真波形

Fig 4 Simulation of arc length

4 结 论

(1) 通过对非线性模型在工作点附近线性化后,采用直接自适应控制算法,通过调节焊接电源输出电压和送丝速度的大小,使焊接电流和电弧长度跟踪参考模型的输出。

(2) 在性能指标中同时引入状态误差和控制增量,使得控制器的静态和动态性能得到改善。

(3) Matlab 仿真显示系统的输出能很好地跟踪参考模型的输出,验证了算法的有效性。

参考文献:

- [1] Essers W G. Heat transfer and penetration mechanism with GMA and plasma(GMA welding) J. Welding Journal 1981 2(61): 37-42.
- [2] Jalili Kharajoo M, Ghobadipour V, Ebrahimirad H. Robust nonlinear control of current and arc length in GMAW systems[J]. // Proceedings of 2003 IEEE Conference on Control Applications, Istanbul, Turkey. IEEE Publisher 2003. 1313-1316.
- [3] Lesnewich A. Control of melting rate and metal transfer in gas shielded metal arc welding (Part I) [J]. Welding Research Supplement 1958 37(8): 343-353.
- [4] 尹怡欣, 孙一康, 舒迪前. 具有二次型性能指标的简单自适应控制算法及其应用[J]. 控制与决策, 2000 2(15): 236-238.
Yin Yixing, Sun Yikang, Shu Diqian. Simple adaptive control algorithm with quadratic performance and its application[J]. Control and Decision 2000 2(15): 236-238.

作者简介: 张 涛,男,1969 年出生,博士研究生,副教授。主要从事工业过程控制和焊接设备的研究,发表论文 12 篇。

Email: zt4@163.com

Abstract The coatings of arc sprayed tin-based alloy was prepared, the coatings and the coating/substrate interface were characterized by scanning electron microscopy, energy dispersive X-ray spectroscopy and X-ray diffraction. Some mechanical properties of the coatings were measured, and an effective way to increase the tensile strength of the coatings was mentioned. The results show that the microstructure of arc sprayed tin-based alloy consists of lots of uniform and fine metal deposits and the intermetallic compounds Cu_6Sn_5 and SnSb in the coatings look like irregular or globular shape. The existence of a bonding layer between the babbitt coating and the cast iron or steel substrate is of benefit to the coating adherence. The coating has a satisfactory performance under the condition of rubbing, which is better than that of cast babbitt.

Key words tin-base babbitt, microstructure, coating, wear

Blowhole and alloy element burning loss of AlMgSi6082 alloy joint welded by argon arc welding TANG Xiaohong, PANG Tao (1. School of Electromechanical Engineering, Central South University of Forestry and Technology, Changsha 410004, China; 2. Zhuzhou Gear Co., Ltd, Zhuzhou 412000, China), P 21—24

Abstract AlMgSi6082 alloys with thickness of 3 mm and 10 mm were respectively welded by TG welding and MIG welding, and the good welded joints without the superficial flaws were obtained. Through the metallographic test to the joints, the type and difference of blowhole in the joints were studied, and the reason for the blowhole difference was analyzed. Through the measurement of ingredient contents of Mg and Si alloying elements, the burning loss rule of Mg and Si by argon arc welding was discovered. The results show that the skin pores, under-shoulder pores, and heart small pores are easy to emerge in the weld by MIG welding. The nearer to heat affected zone, the lower the element burning loss is. The most serious burning loss of Mg and Si elements is in the middle of the weld, and the burning loss of Mg is obviously higher than that of Si. The burning rate of Mg and Si elements is inversely proportional to the arc length by MIG welding.

Key words argon arc welding, aluminum alloy, blowhole, element burning loss

Direct model reference adaptive control of gas metal arc welding process ZHANG Tao, GUI Weihua, WANG Suijun (Information Science and Engineering Institute, Central South University, Changsha 410083, China), P 25—27

Abstract Welding current and arc length will determine the metal transfer, heat input and weld appearance for gas metal arc welding (GMAW). The mathematical model of welding current and arc length is present through the analysis of GMAW welding process. A direct model reference adaptive control based on the quadratic performance index for the GMAW process is designed, and welding current and arc length are controlled by adjusting of welding power source voltage and wire feed speed to

trace the output of the reference model. At the same time, an estimation model is given for indirect measurement of the arc length, which is difficult to detect in the application. The results of simulation show the validity of the control method.

Key words gas metal arc welding, direct model reference adaptive control, arc length estimation

Microstructure and wear property of surface modification layer produced by laser melt injection WC on Q235 steel

LI Fuquan, CHEN Yanbin, LILiJun (State Key Laboratory of Advanced Welding Production Technology, Harbin Institute of Technology, Harbin 150001, China), P 28—32

Abstract Laser melt injection (IMI) technology has great potential in the field of material surface modification. WC powder was injected into the surface of Q235 steel by IMI process, and the influence of process parameters was studied. The microstructure and composition of the coatings were analyzed by means of SEM, XRD and EDS. Hardness and wear resistant property of the coatings was measured. The results show that successful IMI layer can be achieved only on the condition that process parameters meet the strict requirements. Through optimizing the process parameters, excellent coatings can be acquired. Microstructure in the coatings is complex, which consists of WC , W_2C and M_6C ($\text{Fe}_3\text{W}_3\text{C}$ - $\text{Fe}_4\text{W}_2\text{C}$) phases. The differences of $\text{Fe}_3\text{W}_3\text{C}$ microstructure in the different zones of the coatings are obvious. The compositions of the reaction layers around particles and dendrite precipitation carbides in the upper coating are both $\text{Fe}_3\text{W}_3\text{C}$. The average hardness of IMI layer is about four times of that of Q235 steel. The friction coefficient of IMI layer is not over one quarter of that of the substrate, which indicates wear resistance of coatings enhanced sharply.

Key words laser melt injection, WC, microstructure, wear resistant property

Effect of current changes on velocity and temperature profiles of GTAW arc CHENG Manqing, AN Yanli, DU Huayun, WEI Yinghui, FAN Ding (1. College of Materials Science and Engineering, Taiyuan University of Technology, Taiyuan 030024, China; 2. College of Materials Science and Engineering, Lanzhou University of Technology, Lanzhou 730050, China), P 33—37

Abstract A steady two-dimensional axisymmetric model was developed in order to investigate heat and fluid flows in a free burning GTAW arc. The velocity and temperature profiles of the arc on the conditions of different currents were simulated, and the calculated results were compared. The conclusion is that with the increasing of the arc current, the energy transferred to the arc increases also, and all the parameters in the arc enhance, which are well consistent with classical arc theory. The control equations are solved by using a general thermo-fluid-mechanics computer program, PHOENICS (Parabolic hyperbolic or elliptic numerical integration code series) code, which is based on the SIMPLE algorithm.

Key words arc, numerical simulation, different currents